Differential Mobility Separation of Ions Using a Rectangular Asymmetric Waveform

D. Papanastasiou,*,† H. Wollnik,‡ G. Rico,§ F. Tadjimukhamedov,† W. Mueller,† and G. A. Eiceman†

Department of Chemistry and Biochemistry, New Mexico State University, Las Cruces, New Mexico 88003, Physikalisches Institut, Justus-Liebig-Universität Giessen, D-35392 Germany, and Engineering Technology Department, New Mexico State University, Las Cruces, New Mexico 88003

Received: December 13, 2007; In Final Form: February 7, 2008

The performance of a planar differential mobility spectrometer (DMS) is investigated when operated in air at ambient pressure and driven by a rectangular asymmetric waveform, limited to frequencies of <1.2 MHz and voltage pulse amplitudes of <1 kV with steep rise times of the order of ∼15 ns. Independent control of frequency, voltage pulse amplitude, and duty cycle allow for characterizing the DMS in terms of transmission, resolution and separation. The tradeoff between sensitivity and resolution and the effect of duty cycle on instrument performance are demonstrated experimentally. The dependence of ion mobility on the magnitude of the electric field determines the displacement of ions measured by the DC compensation voltage as a function of the duty cycle. Optimum values for the duty cycle exist for the separation of A- and C-type ions, while, B-type ions exhibit a more complex behavior. An analytical expression for describing the effect of duty cycle on the separation of the ions, determined by variations in the compensation voltage, is developed and compared to experimental results obtained in air below 75 Td using estimated alpha parameters for a set of ketones. In this context, errors associated with the calculation of alpha parameters using polynomials of even powers are highlighted.

Introduction

The fast motion of molecular ions in gases as compared to their motion in a condensed phase has established ion mobility as a powerful separation tool, especially in conjunction with mass spectrometry. Differential mobility spectrometry (DMS),[1] also known as field asymmetric ion mobility spectrometry (FAIMS),[2] serves as a post-ionization method for filtering ions in a controlled atmosphere, suppressing chemical noise, separating isobaric mixtures, and characterizing molecular ions based on their mobility ratios.[3]

In DMS, ions entrained in a gas stream oscillate in the presence of a high frequency, periodic, asymmetric waveform that alternates between a high-field and a reversed low-field applied perpendicularly to the direction of flow. Differences in mobility between the alternating field polarities result in a net displacement forcing ions to drift progressively off-axis and discharge on electrodes confining gas flow. For ions of a specific mobility, this displacement can be compensated by a DC voltage. By scanning this compensation voltage at fixed amplitude and waveform frequency, ions are transported through the DMS channel, and a spectrum is generated either by using an electrometer or introducing ions into a mass spectrometer.

The design of the waveform is an essential feature for the overall DMS performance, resulting from the dependence of the mobility of the ions with a time-varying electric field. The characteristics of the waveform alter the periodic displacement and influence resolution, transmission, and separation, parameters investigated using numerical modeling of ion trajectories.[4] Asymmetric waveforms employed for DMS and FAIMS analyses are combinations and/or modifications of sinusoidal patterns and include (a) the sum of a sinusoidal and its phase-shifted harmonic, also known as bisinusoidal,[5,6] (b) clipped displaced sinusoidal,[7,8] and (c) quasi-sinusoidal waveforms.[9] The estimated time necessary for reaching terminal velocity during a transient electric field falls into the picosecond time scale,[10] which suggests that ion velocity and hence displacement and finally separation are sensitive to details of the waveform structure. Analytical considerations show that rectangular waveforms improve ion separation as compared with sinusoidal waveforms.[11] Numerical analyses also indicate that rectangular waveforms offer substantial enhancements in instrument performance in terms of resolution and/or sensitivity.[4]

An essential feature of the asymmetric waveform is its duty cycle, that is, the ratio of the width of the positive or negative pulse and the repetition period. The positive and negative waveform integrals are equal and asymmetry is required for separation,[1] expressed by differences in the compensation voltage required to transport ions through the DMS channel. The ability to separate ions reduces for approximately symmetric waveforms with duty cycles close to 0.5. Poor separation is also expected at the other extreme when duty cycle approaches zero, since in this case the distance traveled by ions during a narrow high-field pulse is minimized and the dependence of mobility on electric field disappears.[6] These two extremes indicate the existence of an optimum duty cycle, and numerical modeling shows that the maximum compensation voltage at which an ion can be found occurs for values where the high voltage pulse is ∼30% of the waveform period.[10] Similar values have been calculated for bisinusoidal, clipped sinusoidal, and rectangular waveforms for optimizing transmission and/or resolution.[4]

* Author to whom correspondence should be addressed. E-mail: dpapanastasiou@gmail.com.
† Department of Chemistry and Biochemistry, New Mexico State University.
‡ Justus-Liebig-Universität.
§ Engineering Technology Department, New Mexico State University.

10.1021/jp711732c CCC: $40.75
Published on Web 03/14/2008

Although numerical modeling has proven useful in designing waveforms operated at a fixed duty cycle, there are no experimental findings to substantiate such predictions. Furthermore, it is not known whether an optimum value exists for all types of ions, independent of waveform characteristics, molecular mass, and structure.

The excessive power load imposed by high frequency, high voltage pulses with steep rise times has hindered the development of electronics that deliver rectangular pulses for driving separations based on differential ion mobility. Separation of ions using a rectangular waveform was first attempted during the early stages of FAIMS development,[12] which was impractical, however, since in these experiments the frequency was limited to 83 kHz and the electrical pulses could only be applied for 16 ms. In the present article, we report on experiments in which high frequency, high voltage rectangular pulses were applied to a planar DMS supplied by an electronic circuit similar to those proposed for driving hyperbolic quadrupole mass filters[13] and more recently used in the three-dimensional ion trap mass spectrometer (IT MS), also know as the digital IT MS.[14] Several aspects of the DMS performance related to the rectangular waveform are addressed. Ions of ketones were used to illustrate the tradeoff between resolution and sensitivity. Excursions of ions in the spectrum measured by variations in the compensation voltage as a function of the duty cycle are demonstrated experimentally. A simple analytical expression for predicting such variations requires known alpha parameters, which describe mobility dependence on the magnitude of the applied electric field.

Theory

The average drift velocity of ions dragged by an electric field through a gas at pressures of ~0.1 Torr or higher is $v_d = KE$, where E is the electric field and K is the "ion mobility" that is characteristic of every molecular or atomic ion in a specific atmosphere at a fixed gas temperature T. At fixed T and gas density N, the ion mobility and, hence, the average drift velocity can be approximated by a sum of even powers of E/N:[15]

$$K(E/N) = K_0[1 + a_2(E/N)^2 + a_4(E/N)^4 + ...] \qquad (1)$$

where $K_0 = K(E_0/N)$ is the ion mobility at low-field conditions. Alphas are reported in units of Td^{-2n} ($1\ \mathrm{Td} = 10^{-21}\ \mathrm{V\ m^2}$) and have no further physical meaning.[3] The nonlinear dependence of K, determined by alpha values, is used to classify ions in three groups.[2,12] For A-type ions, mobility increases monotonically over small regions with E/N and $a_2 > 0$, $a_4 > 0$. Alpha parameters are negative for C-type ions, $a_2 < 0$, $a_4 < 0$, in which case the ion mobility decreases monotonically with E/N. B-type ions exhibit a maximum since $a_2 > 0$ and $a_4 < 0$. In drift-tube ion mobility spectrometry (DT−IMS), defined as a first-order separation technique,[16] the dependence of mobility on electric field is determined directly by experiment.[15] DMS employs alternating electric fields, which establish second-order separation[16] and characterize molecular ions based on their mobility ratios.[6] Methods for extracting alphas from experimental data have been proposed[6,9] and take into consideration the detailed structure of the asymmetric waveform. Published results obtained with different DMS units suggest that alphas are independent of instrumental parameters despite differences in the raw data obtained;[8,17] nonetheless, the procedure for extracting alphas is susceptible to combined errors related to theory and experiment, which complicate the method and make it difficult to ascertain the actual values.

In DMS, the electric field is a time-dependent variable, $E(t)$, and separation of ions is made possible by small variations in ion mobility with E/N. In a planar system driven by a rectangular asymmetric waveform, dipolar electric fields are formed with alternating polarities of different magnitude. As a result, ions are progressively displaced as they drift with different velocities during the high-field, $(E/N)_H$, and low-field, $(E/N)_L$, conditions. Derivation of an analytical expression to quantify this displacement, estimate alpha parameters and further describe the effect of duty cycle on the separation of the ions in the spectrum involves the following steps.

The condition for transporting ions through the channel of a planar DMS requires that there is no net displacement over one period of the asymmetric waveform:

$$\int_0^T K\left(\frac{E(t) + E_C}{N}\right)[E(t) + E_C]\,\mathrm{d}t = 0 \qquad (2)$$

For the ideal case of a rectangular asymmetric waveform, this integral reduces to $K_H(E_H + E_C)T_H + K_L(E_L + E_C)T_L = 0$, where $E_HT_H + E_LT_L = 0$, $E_L < 0$, and $T = T_H + T_L$. Rearranging the last expression and using that, $E_L = -\lambda E_H$, and $\lambda = T_H / T_L$, we obtain:

$$\left(1 + \frac{E_C}{E_H}\right)K_H - \left(1 - \frac{E_C}{\lambda E_H}\right)K_L = 0 \qquad (3)$$

Here, the ion mobility at high- and low-field conditions is defined respectively as:

$$K_H = K_0\left[1 + a_2\left(\frac{E_H}{N}\right)^2\left(1 + \frac{E_C}{E_H}\right)^2 + a_4\left(\frac{E_H}{N}\right)^4\left(1 + \frac{E_C}{E_H}\right)^4 + ...\right] \qquad (4a)$$

$$K_L = K_0\left[1 + a_2\left(\frac{\lambda E_H}{N}\right)^2\left(1 - \frac{E_C}{\lambda E_H}\right)^2 + a_4\left(\frac{\lambda E_H}{N}\right)^4\left(1 - \frac{E_C}{\lambda E_H}\right)^4 + ...\right] \qquad (4b)$$

Rewriting eq 3, we obtain:

$$A_0 + a_2\left(\frac{E_H}{N}\right)^2 A_2 + a_4\left(\frac{E_H}{N}\right)^4 A_4 + ... = 0 \qquad (5)$$

where all A terms are conveniently expressed as polynomials of the parameter $E_C/E_H \ll 1$:

$$A_0 = \left(1 + \frac{1}{\lambda}\right)\left(\frac{E_C}{E_H}\right) \qquad (6a)$$

$$A_2 = 1 - \lambda^2 + 3(1 + \lambda)\left(\frac{E_C}{E_H}\right) + \left(1 + \frac{1}{\lambda}\right)\left(\frac{E_C}{E_H}\right)^3 \qquad (6b)$$

$$A_4 = 1 - \lambda^4 + 5(1 + \lambda^3)\left(\frac{E_C}{E_H}\right) + 10(1 - \lambda^2)\left(\frac{E_C}{E_H}\right)^2 + 10(1 + \lambda)\left(\frac{E_C}{E_H}\right)^3 + \left(1 + \frac{1}{\lambda}\right)\left(\frac{E_C}{E_H}\right)^5 \qquad (6c)$$

An approximate solution for the compensating field can then be derived using eq 5 and neglecting all $(E_C/E_H)^n$ terms for $n > 2$:

$$E_C = -E_H(1-\lambda)\frac{a_2\left(\frac{E_H}{N}\right)^2 + a_4\left(\frac{E_H}{N}\right)^4(1+\lambda^2)}{\frac{1}{\lambda} + 3a_2\left(\frac{E_H}{N}\right)^2 + 5a_4\left(\frac{E_H}{N}\right)^4(1-\lambda+\lambda^2)} \quad (7)$$

The alpha coefficients can be estimated by linear regression of eq 5 if E_C, E_H, N, and λ are known, while eq 7 can be used to predict the effect of λ on E_C. Both tasks are undertaken further below.

Instrumentation

A schematic diagram of the planar DMS and simplified electric circuitry is shown in Figure 1. Two 2 kV, 300 W power supplies (PS1 and PS2) drive the high voltage switch (S) together with a TTL signal that controls frequency and duty cycle. Frequencies in excess of 1 MHz at 1 kV_{0-p} can be delivered to the DMS electrode. Higher frequencies necessary for improving ion transmission limit the pulse amplitude and distort the rectangular shape. The duty cycle of the waveform, defined as the width of the high voltage pulse to the waveform period, $d = T_H/T$, can be varied within 0.2 and 0.8. The positive and negative voltage pulse amplitudes can be controlled independently by the two power supplies driving the switch. In the present study, the waveform at the exit of the switch was applied to the DMS plate through a capacitor removing any dc component. For this configuration, a single power supply was sufficient for controlling the relative amplitudes of the waveform. The low frequency sawtooth voltage, or compensation voltage, was taken from the computer controlled NI Card, amplified, and superimposed on the rectangular waveform. A resistor and inductor connected in series were used to limit the high current associated with the waveform and damp the residual rf protecting the sawtooth amplifier. The superimposed waveforms were applied to one of the DMS plates while the opposite plate remained grounded. Positive and negative ions transported through the alternating dipolar electric field were collected on two plates connected to floating electrometers. Signals were amplified and fed into the data acquisition system.

Air was purified through molecular sieve and served as the carrier gas at flows of ~0.80 L min^{-1}. Sample vapors were introduced at ~0.15 L min^{-1}, so that the total gas flow was less than 1 L min^{-1}. A Teflon sheet was used as a spacer to establish a 0.5 mm gap between the DMS plates. The volume of the channel defined by 15 mm long and 5 mm wide plates is ~37.5 mm^3. At 1 MHz and at gas flows of 1 L min^{-1}, ions traverse the DMS plates in ~2.25 ms and undergo approximately 2000 oscillations. The ion source was ~1 mCi of ^{63}Ni. All experiments were carried out in air at ambient pressure and temperature. The gas pressure in the DMS was estimated at P_1 = 730 Torr using a carrier gas flow of F_1 = 1 L min^{-1}, the conductance of the channel $C \sim 1.132$ L min^{-1}, and a pressure at the exhaust of the channel of P_2 = 660 Torr. Moisture levels were measured by a Panametrics moisture image monitor, and experiments were carried out at ~0.150 ppm_V.

Results and Discussion

Rectangular Waveform. A series of rectangular asymmetric waveforms at different amplitudes and duty cycles were monitored by a 100 MHz Tektronix oscilloscope and are shown in Figure 2. The width, T_H, and the amplitude, V_H, of the high voltage pulse, together with the period, T, are indicated by arrows for the intermediate waveform. Here, the duty cycle is defined as $d = T_H/T$ and the values for the waveforms shown

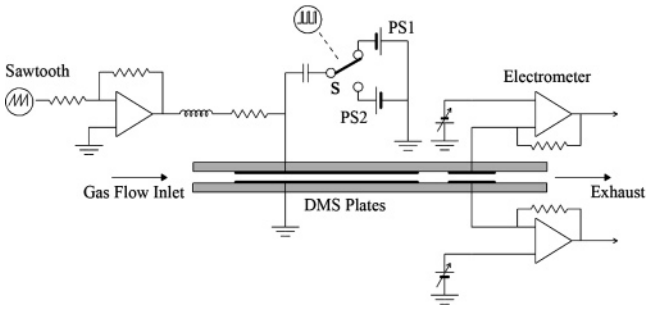

Figure 1. Schematic diagram and simplified circuitry of the switch driving the planar DMS.

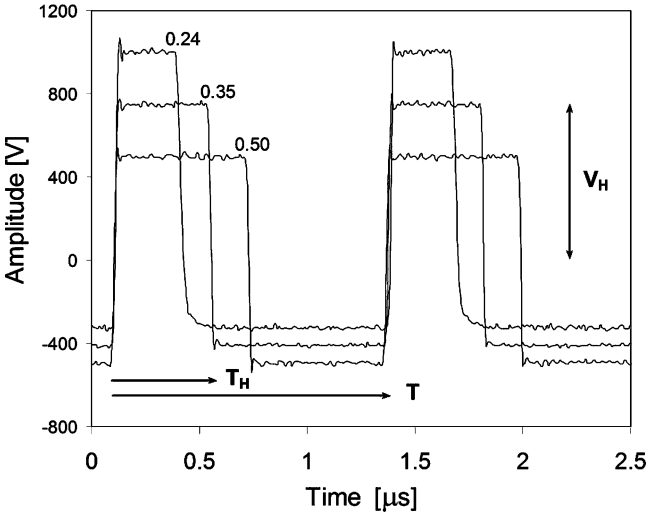

Figure 2. Oscilloscope traces for rectangular asymmetric waveforms at different amplitudes and duty cycles of 0.24, 0.35, and 0.50. Waveforms shown are the average of two oscillograms. Arrows indicate the period of the waveform T, the width of the high voltage pulse T_H, and the amplitude of the pulse V_H.

are d = 0.24, 0.35, and 0.50, all at the same frequency of 0.8 MHz. Duty cycles accessible with current electronics extend from 0.20 to 0.80. Duty cycles below 0.20 or greater than 0.80 distort the rectangular shape and were not investigated. For the waveforms shown, the rise time of the positive pulse is approximately 15 ns, which corresponds to 7% for the narrowest pulses (200 ns) and only 2% for the widest pulses (550 ns). The transition between the high positive pulses and the low negative pulses occurs within less than 50 ns at 0.8 MHz. The maximum voltage for each pulse remains constant to within ~3% resulting in a substantially rectangular high-frequency waveform.

For any given waveform, a dc offset V can be introduced, determined by the following expression:

$$V = (V_H\int_0^{T_H} f(t)\,dt + V_L\int_{T_L}^{T} f(t)\,dt)/T \quad (8)$$

where T_H is the width of the high voltage pulse with maximum amplitude V_H, T_L is the width of the negative pulse with minimum amplitude V_L, $V_L < 0$, and T is the period of the normalized waveform $f(t)$. For the rectangular waveform, eq 8 takes the form:

$$V = V_H d - V_L(1-d) \quad (9)$$

The DC component for the oscillograms shown in Figure 2 has been removed and $V = 0$, since the waveform is fed through

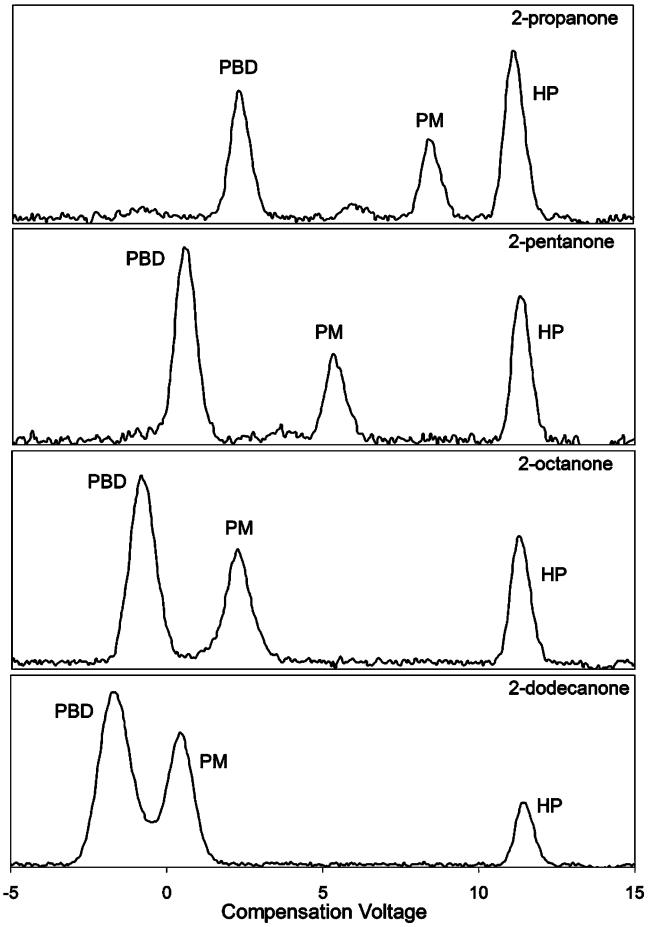

Figure 3. Differential mobility spectra of protonated monomers (PM) of ketones, proton-bound dimers (PBD), and hydrated protons (HP). The waveform operates at 0.8 MHz, $d = 0.30$ and $V_H = 750$ V.

a capacitor. Numerical integration of oscillogram traces gives DC component values of less than 0.01 V.

The performance of the planar DMS driven by the rectangular waveform was tested using a homologous series of ketones. Ketone vapors were introduced through permeation tubes into the main flow of air, and concentrations were adjusted to establish equilibrium conditions between monomer, dimer ions, and hydrated protons. The sample/air flow ratio was set at approximately 2:7. Figure 3 shows the achieved separation for hydrated protons (HP), protonated monomer (PM), and proton-bound dimer (PBD) ions for 2-propanone, 2-pentanone, 2-octanone, and 2-dodecanone. Ions were separated by operating the waveform at a frequency of 0.8 MHz, $d = 0.30$, and $V_H = 750$ V. Hydrated protons appear on the far right of each spectrum at the same compensation voltage of $V_C = 11.4$ V. Proton-bound dimer ions appear on the far left. The low molecular weight 2-propanone exhibits A-type behavior, similar to hydrated protons, for which the mobility increases with V_H and a greater V_C is required to transport ions through the channel. Ion behavior in the DMS driven by a rectangular waveform is examined in more detail by determining alpha parameters below.

Frequency versus Transmission and Resolution. In planar DMS, ion separation is enhanced at the expense of transmission. Ion losses due to greater electric fields can be tolerated by increasing the frequency, which is however limited by the available electronics. Such a tradeoff is reflected by variations of the effective gap, g_e, defined as the width of the channel in the direction of the electric field where ions avoid neutralization on the DMS electrodes.[18] For the following calculations, the

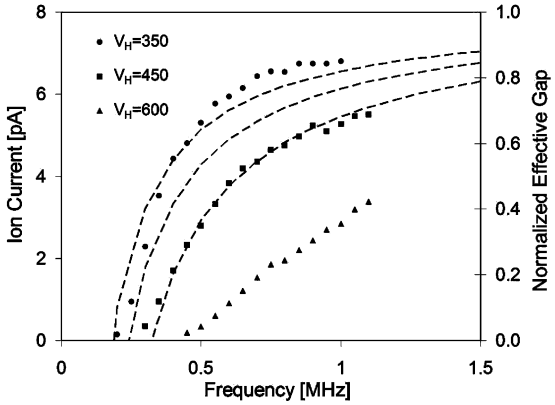

Figure 4. Transmitted ion current as a function of frequency f for three different high voltage pulses, V_H, at 350, 450, and 600 V (dotted curves). At 730 Torr, the corresponding E/N values are 30, 38, and 51 Td. The calculated normalized effective gap g_e is shown on the right axis (dashed curves).

effective gap is expressed by the actual gap between the electrodes, g, reduced by the amplitude of ion oscillation, $g_e = g - 2\delta x$. Approximating δx with the displacement during the high-field only, we obtain

$$\delta x = (V_H/g) \int_0^{T_H} K(E/N) f(t)\, dt \tag{10}$$

and for an ideal rectangular waveform, the effective gap is expressed as

$$g_e = g - \frac{2V_H K_H}{fg}\left(\frac{\lambda}{1+\lambda}\right) \tag{11}$$

where K_H is the ion mobility during the high-field, the pulse-width ratio is $\lambda = T_H/T_L$, and f is the frequency of the waveform. The effective gap is proportional to the transmission of ions and narrows down for higher voltage pulse amplitudes. Such reduced transmission with increasing amplitude is characteristic of the planar configuration where the alternating dipolar electric field exerts no focusing action to the ions. The effective gap is also inversely proportional to the waveform frequency. The effect of these two parameters on ion transmission is determined experimentally for hydrated protons and shown in Figure 4. In this example, the ratio λ is kept constant and transmission is monitored at different voltage pulse amplitudes. Increasing frequency reduces the amplitude of ion oscillation within the DMS channel and intensifies ion current measured at the detector. For the lower amplitude examined, $V_H = 350$, transmission levels-off at ~1 MHz and a frequency of 0.2 MHz is sufficient for transporting ions through the channel. This lower frequency cutoff increases with V_H.

The effective gap, g_e, is proportional to the ion current measured at the end of the DMS channel. Dashed curves in Figure 4 represent the normalized g_e at a frequency of 0.8 MHz, $\lambda = 0.4286$, and the three voltage pulse amplitudes examined experimentally, with corresponding E/N values at 730 Torr of 30, 38, and 51 Td. The mobility coefficients used for hydrated protons in air were 2.14, 2.16, and 2.21 $cm^2\ V^{-1}\ s^{-1}$, respectively.[4] The effective gap is normalized to 0.5 mm, the actual separation between the DMS electrodes, and provides a measure of the improvement anticipated by increasing the frequency of the applied asymmetric waveform. For hydrated protons, the effective gap becomes approximately ~90% of the actual separation gap at a frequency of 1.5 MHz. The calculated lower frequency cutoff appears smaller than that determined

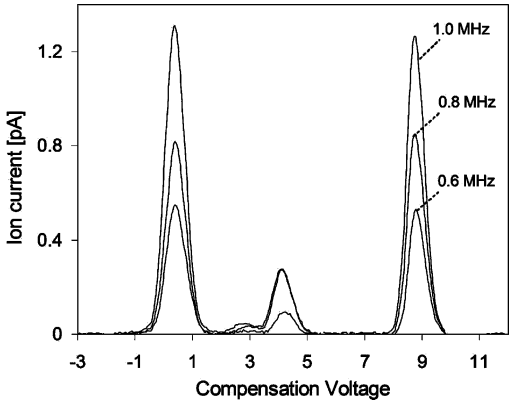

Figure 5. Differential mobility spectra for 2-pentanone protonated monomer (PM) and proton-bound dimer (PBD) ions in equilibrium with hydrated protons obtained at frequencies of 0.6, 0.8, and 1.0 MHz. The duty cycle for all waveforms is $d = 0.30$.

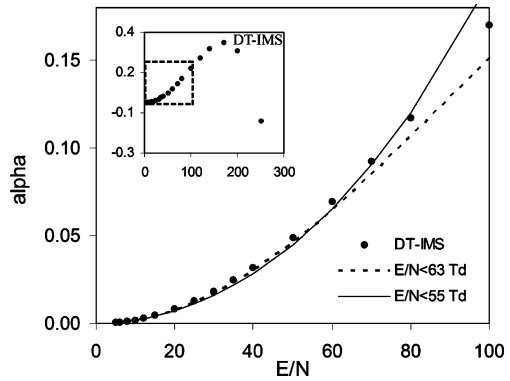

Figure 6. Calculated alpha plot for hydrated oxygen ions using reduced mobility coefficients determined by DT−IMS[19] (see caption) and alpha values determined by DMS employing a rectangular asymmetric waveform and fitting the complete data set up to 63 Td (dashed curve) and part of the data set up to 55 Td (solid curve).

experimentally and can be partially explained by losses due to the fringing fields experienced by the ions prior to entering the pure dipolar electric field. Transmission efficiency is related to the input current; however, space charge effects are known to limit transmission to 10 pA or less.[4]

Figure 5 shows average spectra of 20 scans for 2-pentanone monomer and dimer ions in equilibrium with hydrated protons at waveform frequencies of 0.6, 0.8, and 1.0 MHz at the same $V_H = 690$ V and $d = 0.30$. Frequency enhances transmission but has no effect on ion separation, as suggested by eq 13. Marginal differences in resolution are observed. Ion intensity is lower at reduced frequencies, and the width of the peak at full-width half-maximum for hydrated protons at $V_C = 8.8$ V is $\Delta V_C = 0.68$ V, and $R = 13$. At 1.0 MHz, the width of the peak increases to $\Delta V_C = 0.72$ V, and $R = 12$.

Calculation of Alpha Parameters. Existing data for the reduced mobility of hydrated oxygen ions, $(H_2O)_n \cdot O_2^-$, in air at 300 K obtained by DT−IMS[19] were used as reference to test the accuracy of the method for estimating alphas using the rectangular waveform and eqs 5 and 6. The alpha parameter, expressed as $a = a_2(E/N)^2 + a_4(E/N)^4$, was determined by fitting eq 2 to experimentally determined values for K_0 based on the method of least-squares. The inset in Figure 6 shows DT−IMS data for the alpha parameter plotted as a function of the full measurement range of E/N. Careful analysis of the data showed that accurate fitting was possible up to 120 Td and that eq 2 cannot describe variations of K_0 for the greater E/N values. The alpha parameter is altered significantly when the data range was

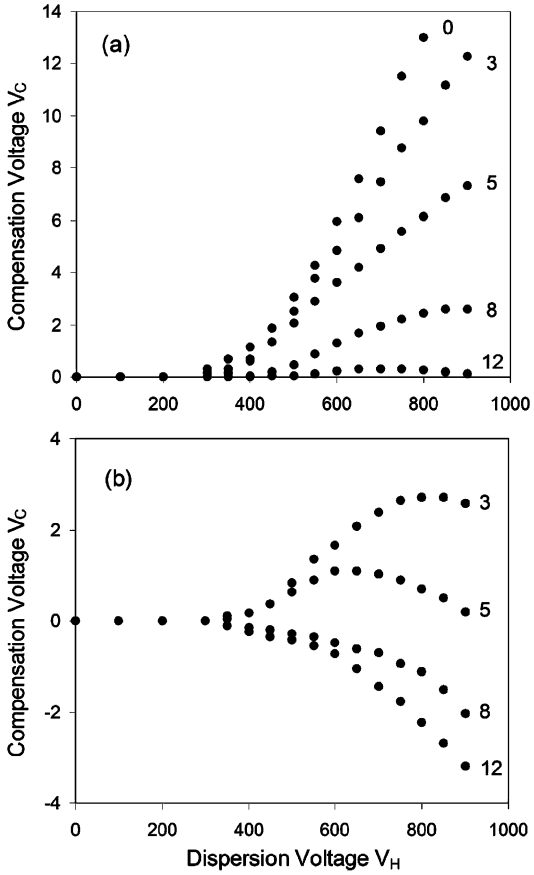

Figure 7. Dispersion curves for protonated ketones (a) and proton-bound dimer ions of ketones (b) showing variations in the compensation voltage V_C as a function of the amplitude of the high voltage pulse, V_H. Curves are labeled with the number of carbons in the molecule, and 0 refers to hydrated protons. Alpha parameters were determined for $d = 0.30$.

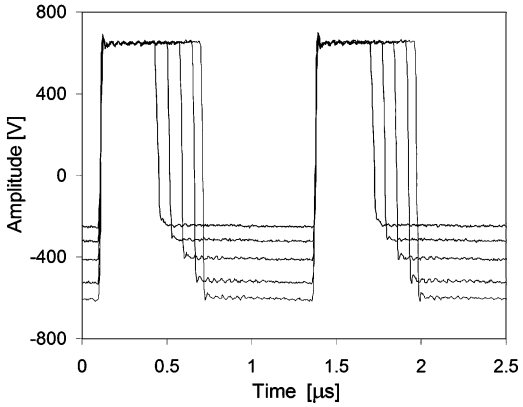

Figure 8. Oscillogram traces of the asymmetric rectangular waveform at different of duty cycles. The frequency is 0.8 MHz and the amplitude of the high voltage pulse is fixed at 650 V. Increasing the duty cycle results in greater negative voltage pulses to balance the areas of the waveform.

reduced, which further demonstrates the limited validity of even power polynomials for describing $K(E/N)$. In this work, curve fitting was extended to $E/N \leq 80$ Td, close to the maximum of 75 Td units accessible with the rectangular waveform at 730 Torr. The estimated values from DT−IMS data are $a_2 = 2.06 \times 10^{-5}$ Td^{-2} and $a_4 = -3.83 \times 10^{-10}$ Td^{-4} at 760 Torr and 300 K.

The alpha parameters in DMS are determined using dispersion curves where the amplitude of the high voltage pulse, V_H, of the applied waveform is plotted over the corresponding position

TABLE 1: Alpha Values for Protonated Ketones and Proton-Bound Ketone Dimers

	protonated monomers			
	2−propanone	2−pentanone	2−octanone	2−dodecanone
formula	$(C_3H_6O)H^+$	$(C_5H_{10}O)H^+$	$(C_8H_{16}O)H^+$	$(C_{12}H_{24}O)H^+$
a_2 ($\times 10^{-5}$)	1.76	1.16	0.52	0.11
a_4 ($\times 10^{-9}$)	−1.05	−0.92	−0.37	−0.13
	proton-bound dimers			
	2−propanone	2−pentanone	2−octanone	2−dodecanone
formula	$(C_3H_6O)_2H^+$	$(C_5H_{10}O)_2H^+$	$(C_8H_{16}O)_2H^+$	$(C_{12}H_{24}O)_2H^+$
a_2 ($\times 10^{-6}$)	7.44	4.33	−1.20	−2.16
a_4 ($\times 10^{-10}$)	−6.94	−7.03	−0.32	−0.84

of the ions in the spectrum, V_C. Alpha values obtained by DMS analysis employing the rectangular waveform at an estimated pressure of 730 Torr and 297 K using all data available (V_H < 750 V, E/N < 63 Td) are $a_2 = 1.93 \times 10^{-5}$ Td^{-2} and $a_4 = -4.30 \times 10^{-10}$ Td^{-4}. The corresponding alpha function is represented by the dashed curve in Figure 6 and shows that DT−IMS and DMS data match for E/N < 50 Td. The difference in the values for a_2 is 6%. The solid curve refers to calculations, which involve fitting part of the data set (V_H < 650 V, E/N < 55 Td). Reducing the range of data used in the fitting procedure does not result in a better match for the alpha parameters obtained.

Dispersion curves for all ions of ketones examined are shown in Figure 7a,b for protonated monomers and proton-bound dimers, respectively. Each curve is labeled with the number of carbons in the molecule. The calculated alpha parameters, a_2 and a_4, expressed in units of Td^{-2} and Td^{-4}, respectively, are given in Table 1. The gas density at 730 Torr and 297 K is approximately $N = 2.373 \times 10^{24}$ m^{-3}, the analytical gap is $g = 0.5$ mm, and $d = 0.30$. Experiments were carried out at moisture levels of ~150 ppm$_V$.

Calculations involving the determination of the alpha parameters are subject to experimental errors, as well as errors related to the method of extracting coefficients using eqs 5 and 6. Experimental errors are associated with accurate determination of the apex obscured by non-Gaussian peak shapes. The rectangular waveform is associated with high current transients as a result of the steep rise and fall times of the voltage pulses applied to the DMS electrode. Such high current transients generate electronic jitter, which results in peak drifting relative to $V_C = 0$. The error introduced by this jitter was estimated to be ±0.2 V. Electronic jitter also causes peak broadening when averaging spectra, necessary for smoothing peak shapes to determine the position of the apex.

Application of eq 2 and consequently eqs 5 and 6 for fitting data is limited and introduces numerical errors, as discussed above for oxygen ions. Alternative expressions have been proposed for fitting DT−IMS data,[20] also applied to FAIMS for chlorine ions in air.[10] Curve fitting becomes especially problematic for B-type ions where ion mobility exhibits a maximum. In addition, in the derivation of eqs 5 and 6 the transition period between the high positive and the low negative voltage pulses was neglected. The accuracy with which alphas are determined using eqs 5 and 6 and fitting the full data range is tested using eq 7 to predict the effect of the duty cycle. The method requires ions with known alphas and compares estimated and experimental results, as discussed below for ketones.

Waveform Duty Cycle. Duty cycle is one of the parameters least explored in DMS and FAIMS systems. Waveforms for driving DMS or FAIMS analyses are usually designed to operate at a fixed $\lambda = T_H/T_L$. The range of values normally used falls within $0.25 < \lambda < 0.50$, which corresponds to duty cycles of $0.20 < d < 0.33$, with $d = \lambda/(1 + \lambda)$.

The fast switch employed in this work is controlled by a TTL signal, and the range of duty cycles available runs between $d = 0.2$ and $d = 0.8$. In planar DMS, the polarity of the waveform has no effect on performance other than reversing the position of the ions relative to $V_C = 0$ V. Therefore, experiments covered only one-half of the available range, that is, from 0.2 to 0.5 V. Results can be extrapolated to higher values by a simple sign reversal in V_C.

The duty cycle of the waveform is investigated by fixing the amplitude of the positive pulse and scanning λ at a fixed frequency. Selected oscillograms of such a scan are shown in Figure 8 for $V_H = 650$ V. The amplitude of the negative voltage pulse increases with duty cycle so that the areas of the waveform remain balanced. Therefore, the effect of d on V_C cannot be investigated independently.

Figure 9a,b shows variations in the position of the ions in the spectrum as a function of the duty cycle for protonated monomer ketones and proton-bound ketone dimers, respectively. Dashed curves with error bars determined experimentally and solid curves calculated analytically using eq 7 are labeled with the number of carbons in the molecule. Error bars indicate maximum and minimum variations in the compensation voltage of the apex for three sets of measurements. The experimental error appears enhanced for the lower duty cycles, which is associated with limitations in electronics distorting the applied asymmetric waveform. Ions identified as A-type exhibit a maximum compensation voltage. The experiment shows that all A-type monomer ions exhibit a maximum excursion from $V_C = 0$ V at approximately $d = 0.33$. In this case, the separation of the ions in the spectrum is maximized and appears independent of the amplitude of the voltage pulse. C-type ions exhibit a minimum at a slightly higher value, $d = 0.38$, as shown by 2-octanone and 2-dodecanone dimer ions in Figure 9b. B-type ions exhibit a more complex behavior with a point of inflection, as shown for the 2-dodecanone monomer and for 2-propanone and 2-pentanone dimer ions. The compensation voltage goes through a maximum for the lower duty cycles to a minimum crossing zero, $V_C = 0$ V. The experimental error for ions with such variations in V_C precludes an absolute determination of a maximum excursion; however, it can be seen that for 2-propanone and 2-pentanone dimer ions the optimum falls around $d = 0.33$ at $V_H = 650$ V.

Solid curves in Figure 9a,b are calculated analytically using eq 7 and the alpha parameters given in Table 1. While the general trend in the theoretical curves matches that of experimental data, in certain cases, the error may reach ±0.3 V, which partially reflects the accuracy of the fitting procedure using eq

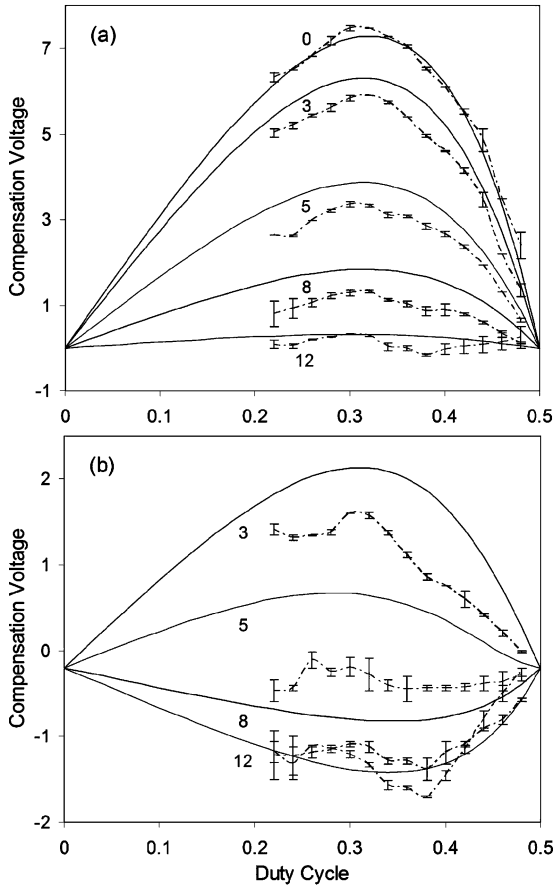

Figure 9. Experimental curves (dashed) with error bars and theoretical curves (solid) of ion position in the spectrum expressed by the compensation voltage V_C as a function of the duty cycle d for protonated ketones (a) and proton-bound ketone dimers (b). Curves are labeled with the number of carbons in the molecule, and 0 refers to hydrated protons.

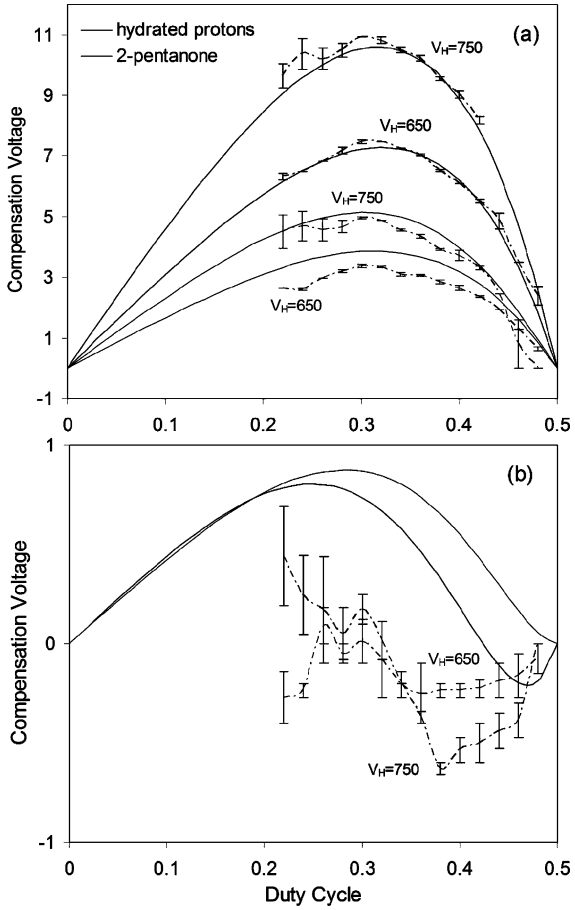

Figure 10. Experimental curves (dashed) with error bars and theoretical curves (solid) of compensation voltage V_C as a function of the duty cycle d for hydrated protons and 2-pentanone monomer ions (a) and proton-bound 2-pentanone dimers (b), at V_H = 650 V and V_H = 750 V.

2. Theoretical curves are extended to $d = 0$, where ions exhibit no mobility dependence, as observed at the other extreme, $d = 0.50$.

Calculations of ion excursions in terms of V_C assumes that the alpha parameters remain constant throughout the range of duty cycles examined experimentally. However, since small variations of alphas do exist as the duty cycle of the waveform is varied,[6] average values may be used instead. In this study, experiments with 2-propanone at duty cycles of 0.25, 0.30, and 0.35 indicated that alphas decrease with d, in accordance with numerical analysis,[6] and that average values can be obtained at $d \sim 0.30$.

Variations in the values of the alpha parameters with duty cycle may partially account for the different alphas reported for ketones using the quasi-sinusoidal waveform[9] and those in Table 1, in addition to differences in the range of E/N used for curve fitting. An example of the importance of choosing the most appropriate range for fitting data is made with reference to Figure 10a, where excursions in V_C by varying d for hydrated protons and 2-pentanone monomer ions are examined at two different amplitudes of V_H = 650 V and V_H = 750 V. Theoretical curves for hydrated protons converge to experimental results by fitting eq 2 using the full data range available. The calculated alpha parameters for hydrated protons are $a_2 = 1.78 \times 10^{-5}$ Td^{-2} and $a_4 = -4.91 \times 10^{-10}$ Td^{-4}. In contrast, the behavior of the B-type 2-pentanone monomers cannot be predicted accurately, even if the data range used in the fitting procedure is reduced. The effect is more pronounced with 2-pentanone proton-bound dimers, shown in Figure 10b for two different voltage pulse amplitudes. Despite the rather large experimental error of the order of ± 0.3 *V*, theoretical curves fail to describe the actual trend. Such observations further demonstrate that eq 2 is limited in describing variations of mobility with electric field.

Conclusions

Differential mobility separation of ions is performed on a planar system driven by a rectangular asymmetric waveform at frequencies of 1.0 MHz or less and voltage pulses amplitudes up to $V_H \sim 1.0$ kV. Experiments demonstrate that the duty cycle of the waveform has a strong influence on ion separation. Ions can be classified into three types, depending on their excursions in terms of compensation voltage V_C versus duty cycle d. These excursions follow the classification of ions based on their mobility variations with electric field. Experimental results and theoretical calculations indicate that optimum operating conditions for enhancing separation, identified as the maximum compensation voltage at which an ion can be found, is a function of the duty cycle and differs for each type of ion. The more complex behavior exhibited by B-type ions suggests that optimum duty cycles may depend on the mixture to be analyzed.

Acknowledgment. The authors are grateful to Professor Alexander Kalimov for insightful discussions. The support of Dr. Sumio Kumashiro and Dr. Shigeru Fukushima is also acknowledged.

References and Notes

(1) Buryakov, I. A.; Krylov, E. V.; Nazarov, E. G.; Rasulev, U. K. *Int. J. Mass Spectrom. Ion Processes* **1993**, *128*, 143.

(2) Purves, R. W.; Guevremont, R.; Day, S.; Pipich, C. W.; Matyjaszcyk, M. S. *Rev. Sci. Instrum.* **1998**, *69*, 4094.

(3) Guevremont, R. *J. Chrom. A* **2004**, *1058*, 3.

(4) Shvartsburg, A. A.; Tang, K.; Smith, R. D. *J. Am. Soc. Mass Spectrom.* **2005**, *16*, 2.

(5) Krylov, E. V. *Tech. Phys.* **1999**, *44*, 113.

(6) Guevremont, R.; Barnett, D. A.; Purves, R. W.; Viehland, L. A. *J. Chem. Phys.* **2001**, *114*, 10270.

(7) Buryakov, I. A.; Kolomiets, Y. N.; Luppu, B. V. *J. Anal. Chem.* **2001**, *56*, 381.

(8) Buryakov, I. A. *Talanta* **2003**, *61*, 369.

(9) Krylov, E.; Nazarov, E. G.; Miller, R. A.; Tadjikov, B.; Eiceman, G. A. *J. Chem. Phys. A* **2002**, *106*, 5437.

(10) Viehland, L. A.; Guevremont, R.; Purves, R. W.; Barnett, D. A. *Int. J. Mass Spectrom.* **2000**, *197*, 123.

(11) Krylov, E. V. *Int. J. Mass Spectrom.* **2007**, *266*, 76.

(12) Guevremont, R.; Purves, R. W. *Rev. Sci. Instrum.* **1999**, *70*, 1370.

(13) Sheretov, E.; Terent'ev, V. *Zh. Tekh. Fiz.* **1972**, *42*, 953.

(14) Ding, L.; Kumashiro, S. *Rapid Commun. Mass Spectrom.* **2006**, *20*, 3.

(15) Mason, E. A., McDaniel E. W. *Transport Properties of Ions in Gases*; Wiley: New York, 1988.

(16) Shvartsburg, A.; Mashkevich, S. V.; Smith, R. D. *J. Chem. Phys.* **2006**, *110*, 2663.

(17) Eiceman, G. A.; Krylov, E.; Krylova, N.; Nazarov, E. G.; Miller, R. A. *Anal. Chem.* **2004**, *76*, 4937.

(18) Krylov, E. V. *Int. J. Mass Spectrom.* **2003**, *225*, 39.

(19) Viehland, L. A.; Mason, E. A. *At. Data Nucl. Data Tables* **1995**, *60*, 37.

(20) Saporoshenko, M. *Phys. Rev. A* **1973**, *8*, 1044.